Optimization of geometric parameters of the standardized multilayer microperforated panel with finite dimension

Xiaocui Yang[a], Liang Chen[a, b], Xinmin Shen[a, c, *], Panfeng Bai[a, *], Sandy To[c], Xiaonan Zhang[a], Zhizhong Li[a]

[a]Department of Mechanical Engineering, College of Field Engineering, Army Engineering University, Nanjing, Jiangsu 210007, China; [b]Automobile NCO Academy, Army Military Transportation University, Bengbu, Anhui 233011, China; [c]State Key Laboratory in Ultra-precision Machining Technology, Department of Industrial and Systems Engineering, The Hong Kong Polytechnic University, Kowloon, Hong Kong SAR, China.

Corresponding author: shenxmjfjlgdx2014@163.com; baipanfeng1990@foxmail.com

Abstract. Standardized multilayer microperforated panel fabricated by laser beam machining of the spring steel was proposed for noise reduction in this study. Geometric parameters of the standardized multilayer microperforated panel, which include diameter of the hole, thickness of the panel, distance between the neighbor holes, and length of the cavity, were optimized for the better sound absorption performance. Sound absorption coefficient of the standardized multilayer microperforated panel was theoretically modeled based on the Maa's theory. The optimization of geometric parameters of the standardized multilayer microperforated panel was obtained by the Cuckoo search algorithm, and the finite dimension of 30 mm was treated as the additional constraint condition. Preliminary verification of the obtained optimal parameters was conducted through the constructed finite element simulation model. Actual sound absorption coefficients of the standardized multilayer microperforated panels with layer number of 1 to 4 were measured by the standing wave method, which were consistent with theoretical data and simulation data, and the corresponding average values in the frequency range of 100-6000 Hz were 57.45%, 70.85%, 71.99%, and 72.28%, respectively. By the theoretical modeling, parameter optimization, simulation, and experimental validation, an effective method was proposed to develop practical sound absorbers, which would promote their applications in noise reduction.

Keywords: standardized multilayer microperforated panel; optimal geometric parameters; sound absorption coefficient; theoretical modeling; finite element simulation; experimental validation.

1. Introduction

Since the basic theory of the microperforated panel was first developed by Prof. Maa in 1975 [1] and further improved in 1988 [2], it is considered as the promising sound absorber for noise reduction in the field of acoustics right now [3], because it has the advantages of a simple structure, high strength, low weight, fine washability, high temperature resistance, outstanding machinability, environmental friendliness, and a low manufacturing cost [4, 5]. Sound absorption performance of microperforated panel is determined by its geometric parameters, which include diameter of the hole, thickness of the panel, distance between the neighbor holes, and length of the cavity. Thus, optimization of geometric parameters of the microperforated panel is the critical step to promote its application [6-9]. Asdrubali et al. [6] had investigated properties of the transparent sound absorbing panel, and the experimental results agreed with the theoretical predictions. Xi et al. [7] had proposed the noise control of dipole source by using microperforated panel housing, and the optimization process had been conducted on several parameters, such as panel mass, bending stiffness, and perforation property. Microperforated absorbers with the incompletely partitioned cavities had been developed by Huang et al. [8], and the results indicated that the appropriately arranged insertion could improve performances of the sound absorber effectively at the low frequency region. Tayong et al. [9] had conducted the inversion of parameters of the microperforated panel by an analytical forward model constructed by the simulated annealing algorithm, and relatively good agreement was found between the experimental data and the model prediction as well as between the inverted parameters and the measured values.

Meanwhile, multilayer microperforated panel has been developed to obtain a better sound absorption performance with wide absorbing band [10-13]. Sui et al. [10] had taken absorbing efficiency of the multilayer microperforated panel as the optimization target and treated the boring rate, aperture, and

cavity depth as the structural parameters based on genetic algorithm. Zhang et al. [11] had conducted optimizations of the multilayer microperforated panel with 3 layers and that with 4 layers, and the results indicated that the absorption coefficient and frequency range were improved remarkably. The acoustic property of multilayer sound absorber with 3D printed microperforated panel was studied by Liu et al. [12], and the results showed that increasing the perforation ratio yielded a higher acoustic resonance frequency for the peak sound absorption coefficient. Sound absorption performance of the multilayer microperforated rib-stiffened panel was studied by Zhou et al. [13], and numerical results indicated that the sound absorption performance of the whole structure was significantly enhanced by perforating the panel with microholes. These studies on parameter optimization of the multilayer microperforated panel were favorable to improve its sound absorption performance.

However, it is considered that there are two major inadequacies of the current research on multilayer microperforated panel, which restrict its application in the wider ranges. Firstly, limit of the available space for installation of the absorber is not taken into account, and optimizations of the parameters only focus on the theoretical value based on mathematical model. It will be better if total thickness of the absorber is limited in a finite dimension, which is favorable to save more space. Secondly, each layer is treated as independent target in optimization of the multilayer microperforated panel, and the parameters of each layer are different. It not only results in the unsatisfactory actual sound absorption coefficient relative to the theoretical result for the fabrication error, but also raises the manufacturing cost. Meanwhile, improvement of the sound absorption coefficient by optimization of the parameters is finite. Along with increase of layers of the multilayer microperforated panel, its space complexity and manufacturing cost are increased gradually, but the promotion efficiency of the sound absorption coefficient is decreased instead, which indicates that the optimization of number of the layers need to

be taken into consideration. Therefore, the optimization of geometric parameters of the standardized multilayer microperforated panel with finite dimension is investigated in this research.

The standardized multilayer microperforated panel with finite dimension means that the parameters of each panel are uniform, and its total thickness is restricted. The parameters of each panel include diameter of the hole, thickness of the panel, and distance between the neighbor holes. Total thickness of the multilayer microperforated panel is equal to summation of the lengths of all the cavities and the thicknesses of all the panels. Through treating finite dimension of the standardized multilayer microperforated panel as the additional constrain condition in the optimization process, the proposed sound absorber will be more practical. Meanwhile, through unifying the geometric parameters of each panel in the standardized multiplayer microperforated panel, the structural complexity and the manufacturing cost of the sound absorber will be reduced. According to these understandings in this research, the theoretical model of sound absorption coefficient of the standardized multilayer microperforated panel was constructed based on Maa's theory [1, 2, 14-16]. Later, the optimization of geometric parameters of the standardized multilayer microperforated panel with the finite dimension was obtained by using the Cuckoo search algorithm [17-20]. Afterwards, the simulation model was built according to the finite element method [21-24], which was a preliminary verification of the obtained optimal geometric parameters. Finally, based on the standing wave method [25-28], experimental validation of the achieved optimal parameter was conducted. Through structural design, theoretical modeling, parameter optimization, finite element simulation, and experimental validation, optimal geometric parameters for the standardized multilayer microperforated panel with the finite dimension were obtained, which would be favorable to improve its sound absorption performance and promote its practical applications in more fields.

2. Theoretical modeling of sound absorption coefficient

Schematic drawing of structure of the standardized multilayer microperforated panel was shown in Fig. 1. Each microperforated panel structure consisted of a panel and a cavity, and the holes in the panel were arranged in square distribution. For a standardized multilayer microperforated panel with n layer, there were altogether $n+3$ geometric parameters, which included the diameter of the hole d, distance between the neighboring hole b, thickness of the panel t, and the length of each cavity D_i $(i=1,2,...,n)$, as shown in the Fig. 1. According to the Maa's theory [1, 2, 14-16], the numerical relationship between sound absorption coefficient of a standardized multilayer microperforated panel with its geometric parameters could be obtained through the transfer matrix method [29-32].

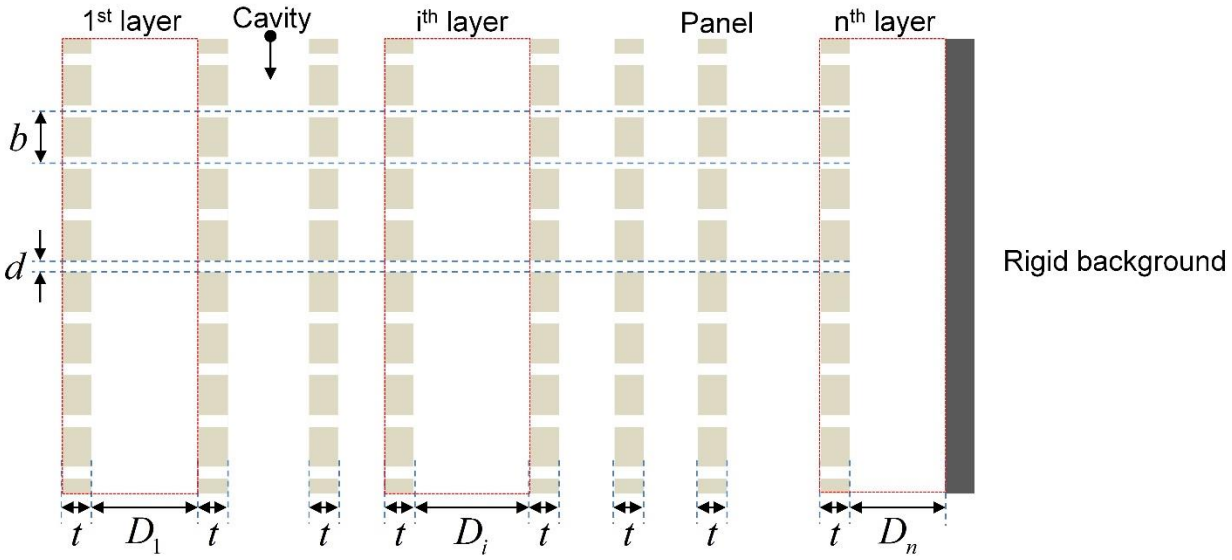

Fig. 1. Schematic drawing of structure of the standardized multilayer microperforated panel

The acoustic impedance Z_s of each microperforated panel was expressed by the Eq. 1. Besides the diameter of the hole d and thickness of the panel t, meanings of the symbols in the Eq. 1 were as follows: μ is the viscosity coefficient of the air, $1.506\bullet10^{-5}$ m^2/s; υ is the temperature conduction coefficient of the metal panel, $2.0\bullet10^{-5}$ m^2/s; ρ is density of the air, 1.225 kg/m^3; ε is perforating rate of the microperforated panel, which can be obtained by the Eq. 2; k_r is the acoustic resistance

constant, which can be derived by the Eq. 3; f is the sound frequency, and its unit is Hz; k_m is acoustic mass constant of the microperforated panel, which can be derived by the Eq. 4; the symbol k in the Eq. 3 and Eq. 4 is the perforated panel constant, and it can be calculated by the Eq. 5 [1, 2, 14-16, 29-32]. Meanwhile, j is the imaginary unit.

$$Z_s = \frac{32(\mu+\upsilon)\rho}{\varepsilon}\frac{t}{d^2}k_r + j\frac{t\rho}{\varepsilon}2\pi f k_m \tag{1}$$

$$\varepsilon = \frac{\pi}{4}\left(\frac{d}{b}\right)^2 \tag{2}$$

$$k_r = \sqrt{1+\frac{k^2}{32}} + \frac{\sqrt{2}}{8}k\frac{d}{t} \tag{3}$$

$$k_m = 1+\frac{1}{\sqrt{9+\frac{k^2}{2}}} + 0.85\frac{d}{t} \tag{4}$$

$$k = \sqrt{\frac{2\pi f}{\mu+\upsilon}}\frac{d}{2} \tag{5}$$

According to the definition in the transfer matrix method, the transfer matrix P_i of the standardized microperforated panel could be calculated by the Eq. 6. Meanwhile, the transfer matrix S_i of the ith layer cavity in the multilayer microperforated panel could be obtained by the Eq. 7, and c in the equation is the acoustic velocity in the air, 340 m/s [1, 2, 14-16, 29-32].

$$[P_i] = \begin{bmatrix} 1 & Z_s \\ 0 & 1 \end{bmatrix} \quad i = 1,2,...,n \tag{6}$$

$$[S_i] = \begin{bmatrix} \cos\left(\frac{2\pi f}{c}D_i\right) & j\rho c\sin\left(\frac{2\pi f}{c}D_i\right) \\ \frac{j}{\rho c}\sin\left(\frac{2\pi f}{c}D_i\right) & \cos\left(\frac{2\pi f}{c}D_i\right) \end{bmatrix} \quad i = 1,2,...,n \tag{7}$$

The total transfer matrix T is the sequential multiplying of transfer matrix P_i of each panel and that S_i of the corresponding cavity, as shown in the Eq. 8. Therefore, according to the Maa's theory

and the transfer matrix method, the sound absorption coefficient α of the standardized multilayer microperforated panel with n layers could be obtained, as shown in the Eq. 9 [1, 2, 14-16, 29-32].

$$[T]=\prod_{i=1}^{n}[P_i][S_i]=[P_1][S_1]...[P_i][S_i]...[P_n][S_n]=\begin{bmatrix}T_{11} & T_{12}\\ T_{21} & T_{22}\end{bmatrix} \tag{8}$$

$$\alpha=\frac{4\,\mathrm{Re}\left(\dfrac{T_{11}}{\rho c T_{21}}\right)}{\left[1+\mathrm{Re}\left(\dfrac{T_{11}}{\rho c T_{21}}\right)\right]^2+\left[\mathrm{Im}\left(\dfrac{T_{11}}{\rho c T_{21}}\right)\right]^2} \tag{9}$$

3. Constrained optimization of geometric parameters

The optimization of geometric parameters of the standardized multilayer microperforated panel with finite dimension aimed to obtain optimal average sound absorption coefficient in certain frequency range $[f_{\min}, f_{\max}]$, which was presented by the Eq. 10. Here $f_{\min}$ is low limit and $f_{\max}$ is upper limit of the investigated frequency range. Meanwhile, there were two constraint conditions for the optimization. Firstly, geometric parameters of the standardized multilayer microperforated panel with n layers must meet requirements of the common microperforated panel [1, 2, 14-16, 29-32], which were presented in the Eq. 11. Secondly, total thickness of the multilayer microperforated panel L was equal to summation of lengths of all the cavities and thicknesses of all the panels, as shown in Eq. 12, which must be smaller than limit of the available space L_0 for installing the sound absorber.

$$\text{maximize}: average\left(\alpha(f)\right) \quad f\in[f_{\min}, f_{\max}] \tag{10}$$

$$\begin{cases} 1\times10^{-4}m \le d \le 1\times10^{-3}m \\ 1\times10^{-4}m \le t \le 2\times10^{-3}m \\ 1\times10^{-3}m \le b \le 1\times10^{-2}m \\ D_i \ge 0 \quad i=1,2,...,n \end{cases} \tag{11}$$

$$L=\sum_{i=1}^{n}\left(t_i+D_i\right)=nt+\sum_{i=1}^{n}\left(D_i\right)\le L_0 \tag{12}$$

According to the obtained theoretical model of the sound absorption coefficient, optimization target,

and the constraint condition, the optimization of geometric parameters of the standardized multilayer microperforated panel with finite dimension was conducted by using the Cuckoo search algorithm [17-20, 33]. Cuckoo search algorithm is founded according to the obligate brood parasitic behavior of some cuckoo species in combination with the Levy flight behavior of some birds and fruit flies. The Cuckoo search algorithm has been proved effective in solving continuous optimization problem. The Cuckoo search is summarized around the following ideal rules: (1) Each cuckoo lays one egg at a time and selects a nest randomly; (2) The best nest with the highest quality egg can pass onto the new generations; (3) The number of host nests is fixed, and the egg laid by one cuckoo can be discovered by the host bird with a probability $p_a \in [0,1]$ [17-20, 33]. For a given bird's nest i and a certain generation t, a new solution $x_i^{(t+1)}$ is generated from the solution $x_i^{(t)}$ according to the Levy flight research mechanism, as shown in Eq. 13 [17-20, 33].

$$x_i^{(t+1)} = x_i^{(t)} + \alpha \oplus Levy(s,\lambda) \tag{13}$$

Here $\alpha(\alpha > 0)$ is the step size, and $\alpha = O(1)$ can be used in many common cases; $Levy(s,\lambda)$ is the step length, which follows the Levy distribution, as shown in the Eq. 14; the symbol $\oplus$ means entry-wise multiplication; s in the Eq. 14 is the step size drawn from Levy distribution [17-20, 33].

$$Levy(s,\lambda) \sim s^{-\lambda}, (\lambda \in (1,3]) \tag{14}$$

Pseudo codes of the standard cuckoo search algorithm were shown in Table. 1. In the optimization of geometric parameters of the standardized multilayer microperforated panel with finite dimension, the target was to maximize average sound absorption coefficient $average(\alpha(f))$ in a certain frequency range $[f_{\min}, f_{\max}]$, as shown in the Eq. 10. The objective function was the Eq. 9, which numerically described the relationship between the sound absorption coefficient $\alpha(f)$ and the frequency f. The three idealized rules in standard Cuckoo search algorithm can be transformed into

the following search methodologies: (1) An egg represents a potential solution and is stored in a nest. Meanwhile, each nest has only a single egg, and a new solution is generated randomly and it replaces a randomly selected nest; (2) The best solution is carried over to the next iteration, which can be judged from the objective function; (3) The host/nest can discover the worse solutions and may discard it and replace it by a new solution, and the probability of discovery is related to the similarity of the solution to the existing solution [17-20, 33]. Based on this Cuckoo search algorithm, the optimization of parameters of the standardized multilayer microperforated panel could be obtained, as shown in Table. 2.

Table. 1 Pseudo codes of the standard Cuckoo search algorithm [17-20, 33]

Standard Cuckoo search algorithm
1: Objective function $f(x), x=(x_1, x_2, ..., x_d)^T$;
2: Generate initial population of n host nests $x_i (i=1,2,...,n)$;
3: **while** ($t \le MaxGeneration$) or (stop criterion) **do**
4: Get a cuckoo (say, i) randomly and generate a new solution by Levy flights;
5: Evaluate its quality/fitness F_i;
6: Choose a nest among n (say, j) randomly;
7: **if** ($F_i \ge F_j$) **then**
8: replace j by the new solution;
9: **end if**
10: A fraction (P_a) of worse nests are abandoned and new ones are built at new locations;
11: Keep the best solutions (or nests with quality solutions);
12: Rand the solutions and find the current best;

13: **end while**

14: Postprocess results and visualization;

Table. 2 Optimization results of geometric parameters based on standard Cuckoo search algorithm

Multilayer	Layer series	Diameter of the hole (mm)	Thickness of the panel (mm)	Distance of the hole (mm)	Length of the cavity (mm)	Optimal average sound absorption coefficient (%)
1	1	0.149	0.100	1.000	16.957	69.79
2	1	0.169	0.100	1.000	13.576	79.40
	2	0.169	0.100	1.000	16.207	
3	1	0.182	0.101	1.004	13.053	82.54
	2	0.182	0.101	1.004	0.425	
	3	0.182	0.101	1.004	16.180	
4	1	0.191	0.101	1.009	12.676	82.62
	2	0.191	0.101	1.009	0.949	
	3	0.191	0.101	1.009	1.451	
	4	0.191	0.101	1.009	14.498	
5	1	0.196	0.101	1.000	11.338	82.74
	2	0.196	0.101	1.000	2.372	
	3	0.196	0.101	1.000	6.371	
	4	0.196	0.101	1.000	0.116	
	5	0.196	0.101	1.000	9.212	
6	1	0.212	0.114	1.053	11.596	83.18
	2	0.212	0.114	1.053	0.803	
	3	0.212	0.114	1.053	7.151	

	4	0.212	0.114	1.053	1.602	
	5	0.212	0.114	1.053	0.257	
	6	0.212	0.114	1.053	7.900	
7	1	0.210	0.126	1.041	10.406	83.43
	2	0.210	0.126	1.041	1.580	
	3	0.210	0.126	1.041	9.527	
	4	0.210	0.126	1.041	1.009	
	5	0.210	0.126	1.041	0.581	
	6	0.210	0.126	1.041	0.484	
	7	0.210	0.126	1.041	5.527	
8	1	0.216	0.110	1.116	11.214	83.57
	2	0.216	0.110	1.116	1.006	
	3	0.216	0.110	1.116	5.125	
	4	0.216	0.110	1.116	3.630	
	5	0.216	0.110	1.116	1.428	
	6	0.216	0.110	1.116	1.019	
	7	0.216	0.110	1.116	1.192	
	8	0.216	0.110	1.116	4.465	

It could be found from the optimization results in Table 2 that the optimal average sound absorption coefficient was improved from 69.79% to 83.57% along with the layer number rose from 1 to 8, but the increase was gradually reduced from 9.61% to 0.14%. Meanwhile, it was interesting to note that the obtained optimal diameter of the hole, thickness of the panel, and the distance of the hole were almost gradually increasing along with adding the layer number. The optimization results exhibited

the effectiveness and reliability of the standard Cuckoo search algorithm.

For the standardized multilayer microperforated panel with different layer numbers, evolutions of the theoretical sound absorption coefficients along with increase of the frequency were shown in Fig. 2, which were consistent with the results in the Table. 2. It could be found that each layer corresponded with a sound absorption peak, and their superpositions formed sound absorption performance of the multilayer microperforated panel [29-32]. That was the major reason for improvement of the sound absorption coefficient along with increase of the layer number, especially in the high frequency band. Meanwhile, it could also be observed that undulations of the sound absorption coefficients were cut down when the layer number increased. Especially when the layer number was larger than 3, the minimum sound absorption coefficient in the frequency range of 1300-6000 Hz exceeded 85%.

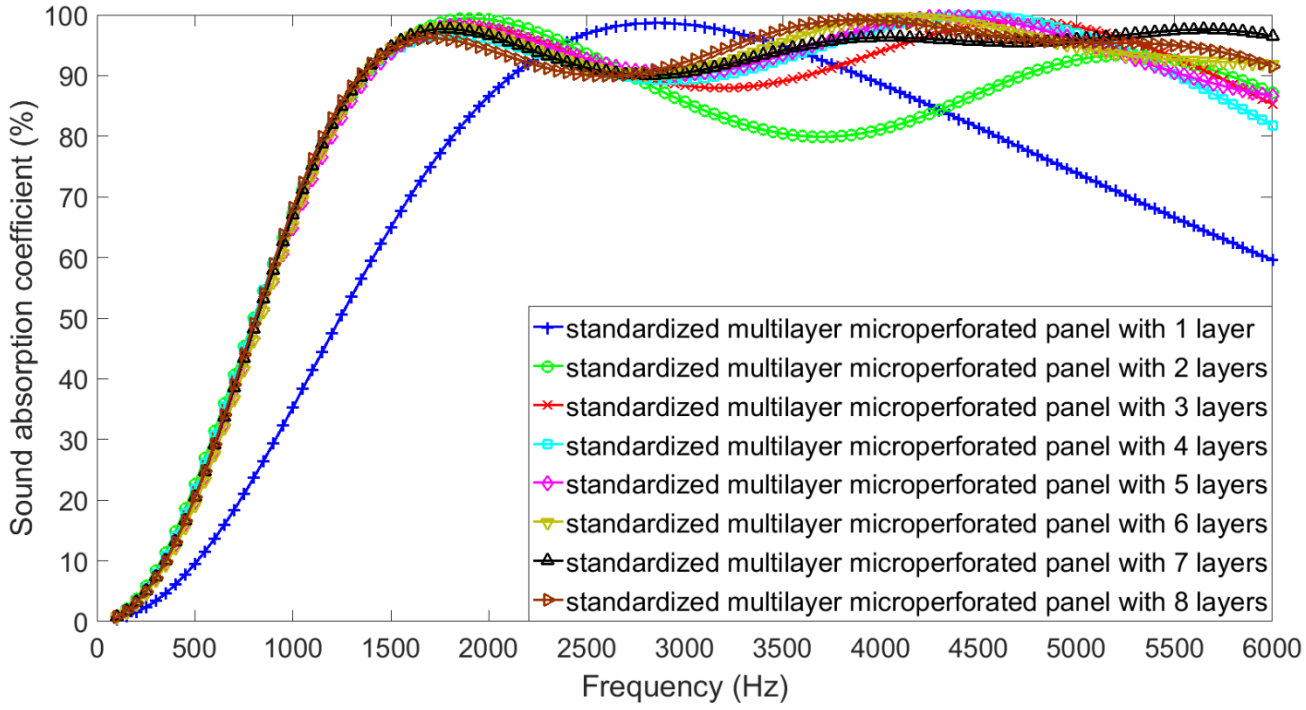

Fig. 2. Evolutions of theoretical sound absorption coefficients along with increase of the frequency

Sound absorption peaks of the multilayer microperforated panels with the different layer number were summarized in the Table. 3. It could be observed that for the multilayer microperforated panel with the layer of 2-8, first peak frequency gradually decreased from 1900 Hz to 1700 Hz, and second

peak frequency declined from 5250 Hz to 3900 Hz, which indicated that the sound absorption peak shifted to the lower frequency direction along with the increase of the layer number. These results were consistent with sound absorption principles of the multilayer microperforated panel [29-32].

Table. 3 The sound absorption peaks of the multilayer microperforated panel with different layer

Multilayer	Peak series	Peak frequency	Corresponding sound absorption coefficient
1	1	2850 Hz	98.69%
2	1	1900 Hz	99.46%
	2	5250 Hz	93.35%
3	1	1850 Hz	98.36%
	2	4700 Hz	98.87%
4	1	1800 Hz	96.81%
	2	4450 Hz	99.98%
5	1	1850 Hz	98.21%
	2	4350 Hz	99.73%
6	1	1800 Hz	98.05 %
	2	4150 Hz	99.71%
7	1	1800 Hz	97.67%
	2	4050 Hz	96.27%
	3	5650 Hz	97.58%
8	1	1700 Hz	96.18%
	2	3900 Hz	99.21%

4. Finite element simulation of optimal parameters

Taking the standardized multilayer microperforated panel with layer number of 4 for example, the simulation model of the optimal parameters obtained by the standard Cuckoo search algorithm was conducted in the software LMS Virtual Laboratory according to the finite element method [21-24], as shown in the Fig. 3(a). Taking the simulation requirements into account, parameter of the multilayer microperforated panel was held two decimal places in the simulation process, as shown in the Table. 4. Plane wave was added on the acoustic source inlet and treated as the sound source input. Two microphones were installed on the standing wave tube to measure the sound pressure of the incident wave and that of the reflected wave, which was used to calculate the sound absorption coefficient for a certain frequency according to the transfer function method. The lengths of the cavity 1, cavity 2, cavity 3, and cavity 4 in Fig. 3(a) were consistent with the data in Table. 4. The 4 microperforated panels were represented by the corresponding transfer relation admittances between the two surfaces, which were determined by the geometric parameters in the Table. 4. Through this method, real part of the sound pressure at the microphone 1 and that at the microphone 2 could be obtained, as shown in the Fig. 3(b). Similarly, imaginary part of the sound pressure at the microphone 1 and that at the microphone 2 could also be obtained, as shown in the Fig. 3(c). According to computational formula of the sound absorption coefficient, sound absorption performances of the standardized multilayer microperforated panel with 4 layers could be obtained. Similarly, the simulations of sound absorption performances of the standardized multilayer microperforated panel with the other layer number were conducted. Therefore, the obtained optimal average sound absorption coefficients for different layers were summarized in the Table. 4. Evolutions of the simulated sound absorption coefficients along with increase of the frequency were shown in the Fig. 4, and they were compared with the results achieved in the theoretical modeling process.

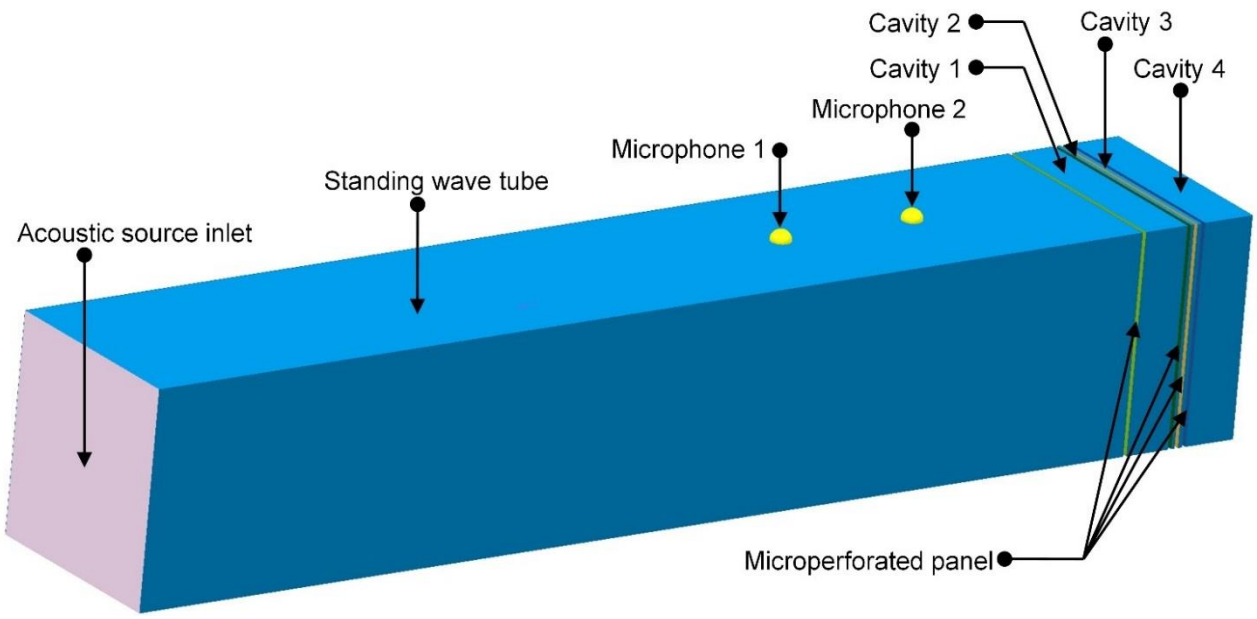

(a) The finite element simulation model

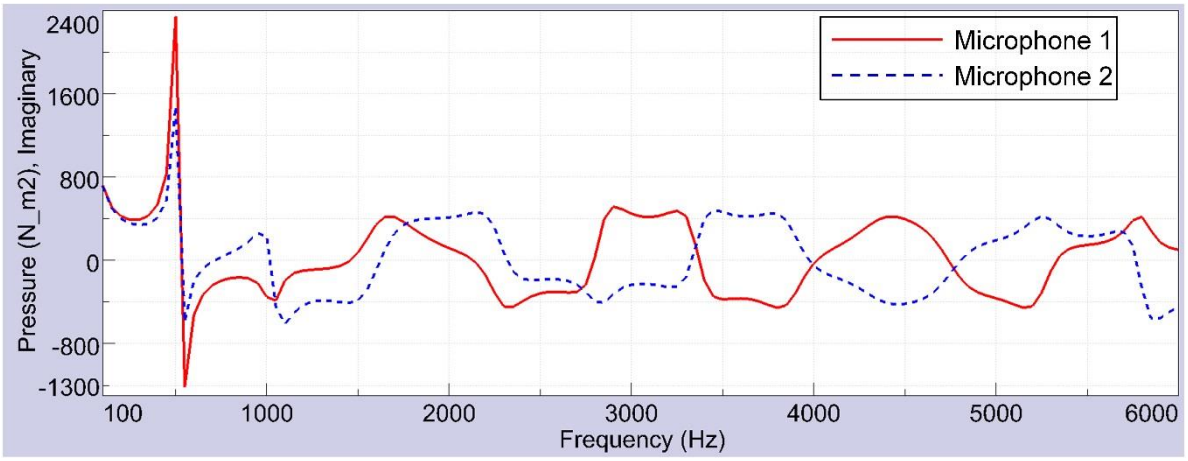

(b) Real part of the sound pressure

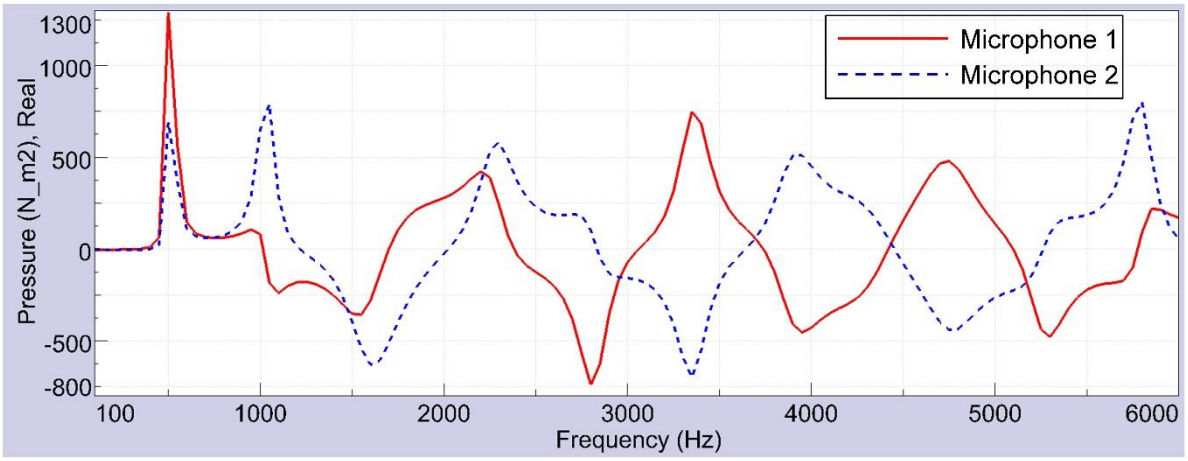

(c) Imaginary part of the sound pressure

Fig. 3. Finite element simulation of the standardized multilayer microperforated panel with 4 layers

Table. 4 Simulation parameters and the obtained optimal average sound absorption coefficients

Multilayer	Layer series	Diameter of the hole (mm)	Thickness of the panel (mm)	Distance of the hole (mm)	Length of the cavity (mm)	Optimal average sound absorption coefficient (%)
1	1	0.15	0.10	1.00	16.96	69.97
2	1	0.17	0.10	1.00	13.58	79.51
	2	0.17	0.10	1.00	16.21	
3	1	0.18	0.10	1.00	13.05	82.68
	2	0.18	0.10	1.00	0.42	
	3	0.18	0.10	1.00	16.18	
4	1	0.19	0.10	1.01	12.68	82.75
	2	0.19	0.10	1.01	0.95	
	3	0.19	0.10	1.01	1.45	
	4	0.19	0.10	1.01	14.50	
5	1	0.20	0.10	1.00	11.34	82.63
	2	0.20	0.10	1.00	2.37	
	3	0.20	0.10	1.00	6.37	
	4	0.20	0.10	1.00	0.12	
	5	0.20	0.10	1.00	9.21	
6	1	0.21	0.11	1.05	11.60	83.21
	2	0.21	0.11	1.05	0.80	
	3	0.21	0.11	1.05	7.15	
	4	0.21	0.11	1.05	1.60	
	5	0.21	0.11	1.05	0.26	
	6	0.21	0.11	1.05	7.90	
7	1	0.21	0.13	1.04	10.41	83.47
	2	0.21	0.13	1.04	1.58	
	3	0.21	0.13	1.04	9.53	
	4	0.21	0.13	1.04	1.01	
	5	0.21	0.13	1.04	0.58	
	6	0.21	0.13	1.04	0.48	
	7	0.21	0.13	1.04	5.53	
8	1	0.22	0.11	1.12	11.21	83.65
	2	0.22	0.11	1.12	1.01	
	3	0.22	0.11	1.12	5.13	
	4	0.22	0.11	1.12	3.63	
	5	0.22	0.11	1.12	1.43	
	6	0.22	0.11	1.12	1.02	
	7	0.22	0.11	1.12	1.19	
	8	0.22	0.11	1.12	4.46	

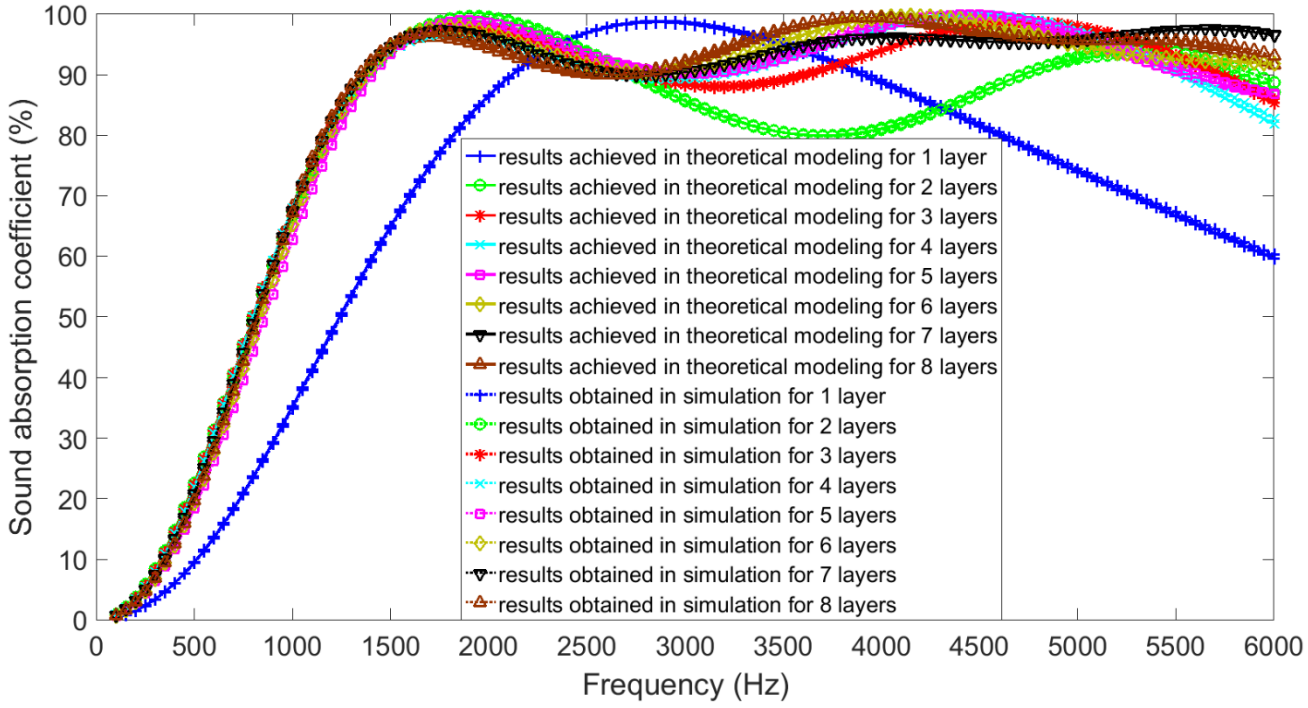

Fig. 4. Comparisons of the results obtained in simulation and those achieved in theoretical modeling

From Fig. 4 it could be found that the results obtained in the simulation were consistent with those achieved in the theoretical modeling. Meanwhile, through comparing the optimal average sound absorption coefficients achieved in the theoretical modeling in the Table. 2 and those obtained in the simulation in the Table. 4, it could further be concluded that these two results were well coincident. Absolute deviations between the results obtained in simulation and those achieved in theory were summarized in Table. 5. It could be found that the deviations were reduced in 2.5% and their average was 0.3415%, which preliminarily verified accuracy of the optimal geometric parameters.

Table. 5 Absolute deviations between the results obtained in simulation and those achieved in theory

layers / Deviations	2 layers	3 layers	4 layers	5 layers	6 layers	7 layers	8 layers
Maximum	0.6587%	1.5966%	0.6882%	1.0090%	2.2695%	0.3181%	0.6988%
Minimum	0.0038%	0.0124%	0.0014%	0.0004%	0.0018%	0.0001%	0.0032%
Average	0.3486%	0.4217%	0.2250%	0.2157%	0.7560%	0.1093%	0.1649%

5. Experimental validation of optimal samples

According to the optimal geometric parameters obtained by the standard Cuckoo search algorithm, the standardized multilayer microperforated panels were fabricated by laser beam machining of the spring steels. It could be judged from Table 2 and Table 4 that improvement of the optimal average sound absorption coefficient was tiny when the layer number was larger than 3. Therefore, the actual sound absorption coefficients of the standardized multilayer microperforated panels with the layer numbers from 1 to 4 were detected, which aimed to validate effectiveness of the optimization. The detection was realized by the AWA6128A detector (Hangzhou Aihong instruments Co., Ltd, China), as shown in Fig. 5 [25, 28]. The detected sample was installed in the sample fixer and fastened by the sample holder. Audio power signal was inputted to the loudspeaker, which was treated as the acoustic source in the standing wave tube. The detected acoustic signal was achieved through the acoustic probe and outputted to the data processer. The pickup was fixed on the pulley, which could move smoothly on the slideway to adjust position of the acoustic probe. The obtained initial experimental data included the peak value $L_{\max}$ and valley value $L_{\min}$ of the sound pressure level for a certain frequency. According to the computational formula of Eq. 15 in the calculation software, the sound absorption coefficient α of the detected sample could be obtained. Meanwhile, detection accuracy of the sound absorption coefficient was determined by diameter of the detected sample. Thus, the detection of sound absorption coefficients in the frequency range of 100-6000 Hz was divided into two-steps [25, 28]. Sound absorption coefficients in 100-1800 Hz and those in 2000-6000 Hz were detected by sample with diameter of 96 mm and by sample with diameter of 30 mm, respectively.

$$\alpha = \frac{4\square 10^{\frac{L_{\max}-L_{\min}}{20}}}{\left(1+10^{\frac{L_{\max}-L_{\min}}{20}}\right)^2} \tag{15}$$

(a) Actual picture

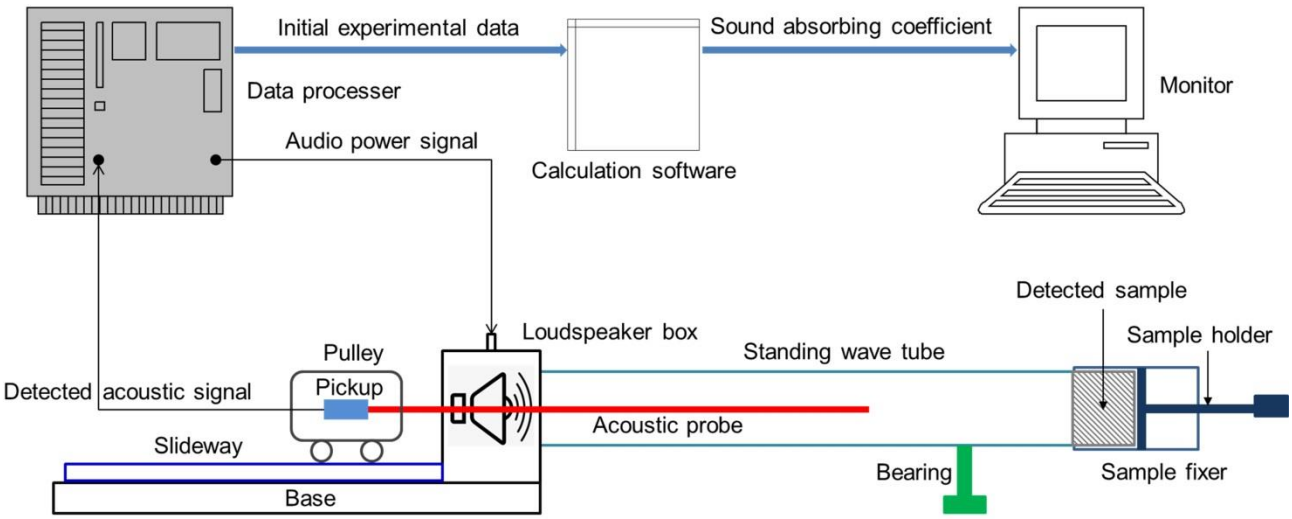

(b) Schematic diagram

Fig. 5. The experimental system for sound absorption coefficient measurement

The actual sound absorption coefficients of the standardized multilayer microperforated panels with the layer numbers from 1 to 4 were shown in Fig. 6. Through the comparisons of sound absorption coefficients of the standardized multilayer microperforated panels in theoretical calculation and those in actual experiment, it could be observed that these two had good consistence and coherence, which could further validate accuracy of the optimization process. Absolute deviations between the results

obtained in experiment and those achieved in theory were summarized in Table 6, and the average absolute deviation between the experimental data and the theoretical data was 6.09%. This deviation was generated by the theoretical errors in the modeling and optimization process, dimensional errors of the fabricated microperforated panels, and the test errors in the measuring program. Besides, the vibration of microperforated panel under the acoustic excitation could result in errors as well. In addition, when two microperforated panels were too close to each other, the plane wave assumption in between might break and bring in more errors, which could be judged from the obvious increase of the deviations in the Fig. 6(c) for the standardized multilayer microperforated panel with 3 layers. Although these errors were unavoidable, some methods had been adopted to reduce their influences. Derivation of the theoretical model according to the Maa's theory and optimization of the geometric parameters based on the cuckoo search algorithm were conducted repeatedly to avoid the calculation error. Ultraprecision laser beam machining was used to manufacture the used microperforated panels, which aimed to reduce the fabrication error. Detections of the sound absorption coefficients by the experimental system in Fig. 5 were conducted many times to reduce the accidental error. It could be calculated that actual average sound absorption coefficients in the frequency range of 100-6000 Hz were 57.45%, 70.85%, 71.99%, and 72.28%, respectively, which corresponded to the proposed standardized multilayer microperforated panels with the layer numbers from 1 to 4. Although the average sound absorption coefficients obtained in experiment were smaller than those achieved in theoretical modeling, this achieved sound absorption performance with finite dimension of 30 mm was satisfying and valuable. In this way, an effective method to develop sound absorber with finite dimension for high sound absorption performance was proposed.

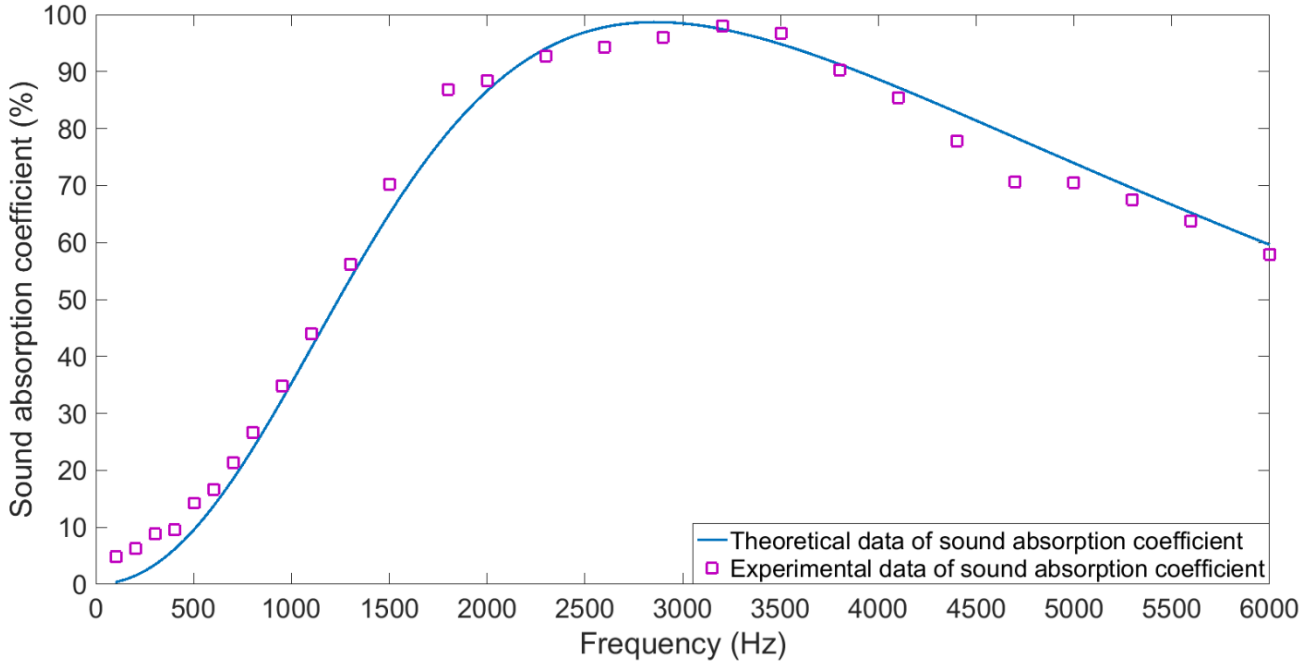

(a) Standardized microperforated panel with 1 layer

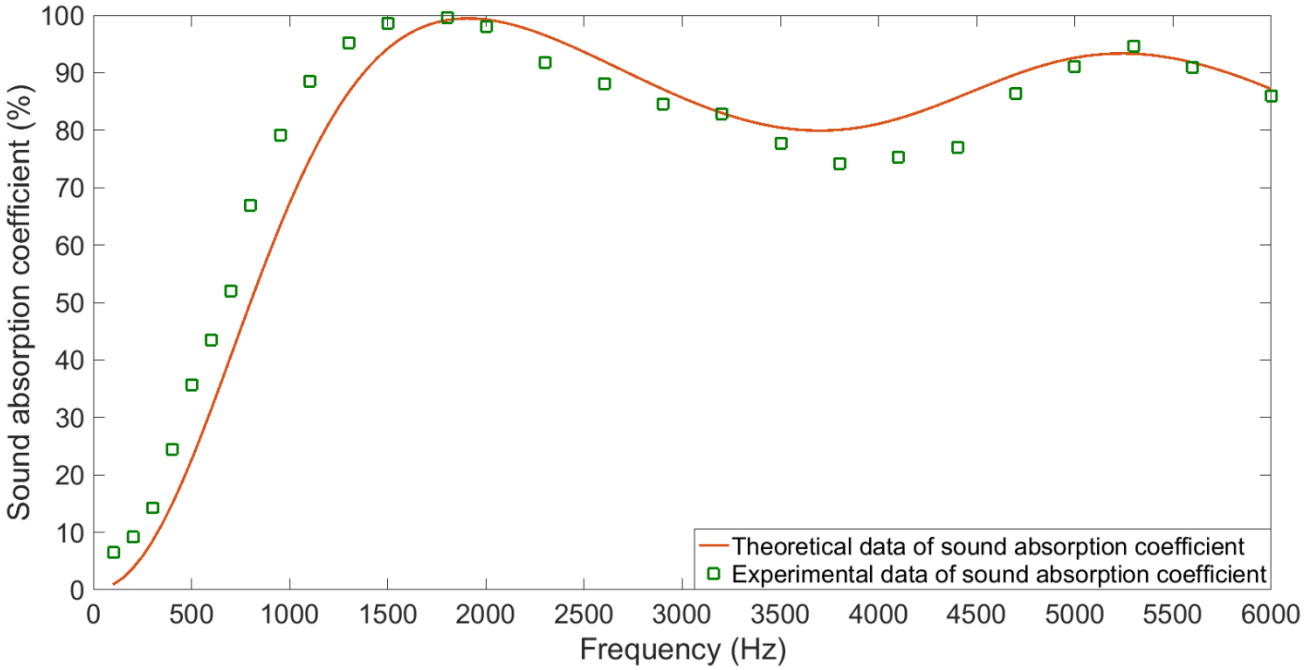

(b) Standardized multilayer microperforated panel with 2 layers

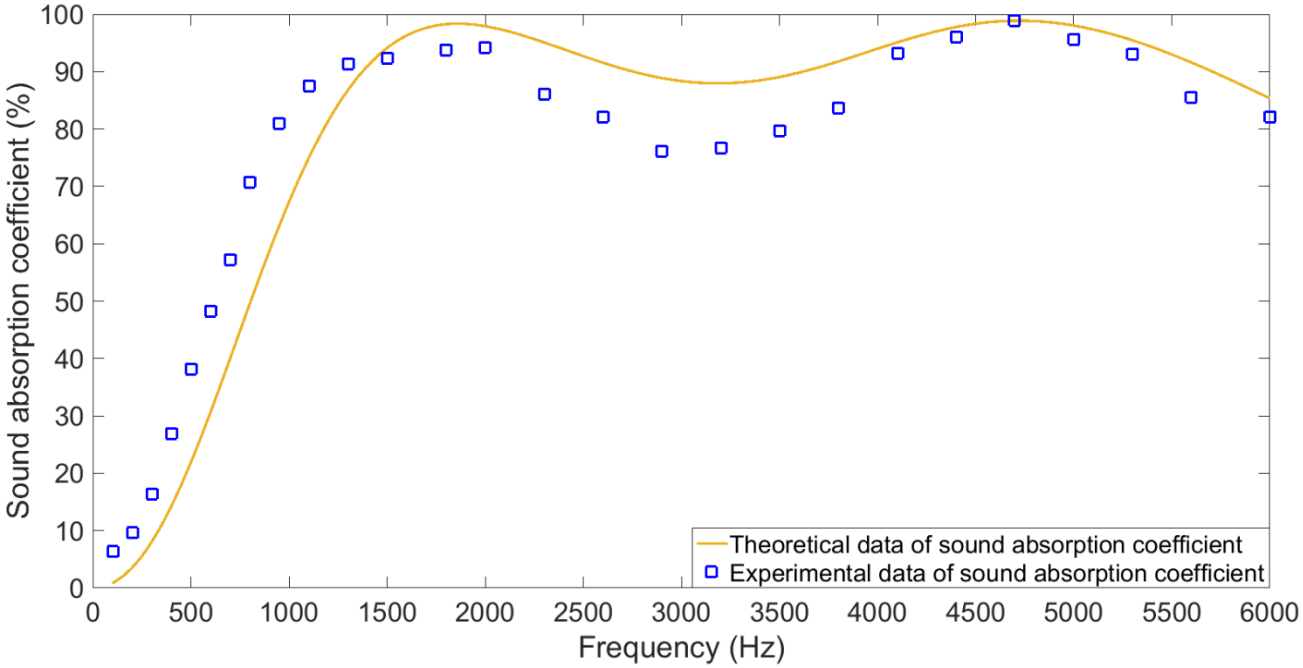

(c) Standardized multilayer microperforated panel with 3 layers

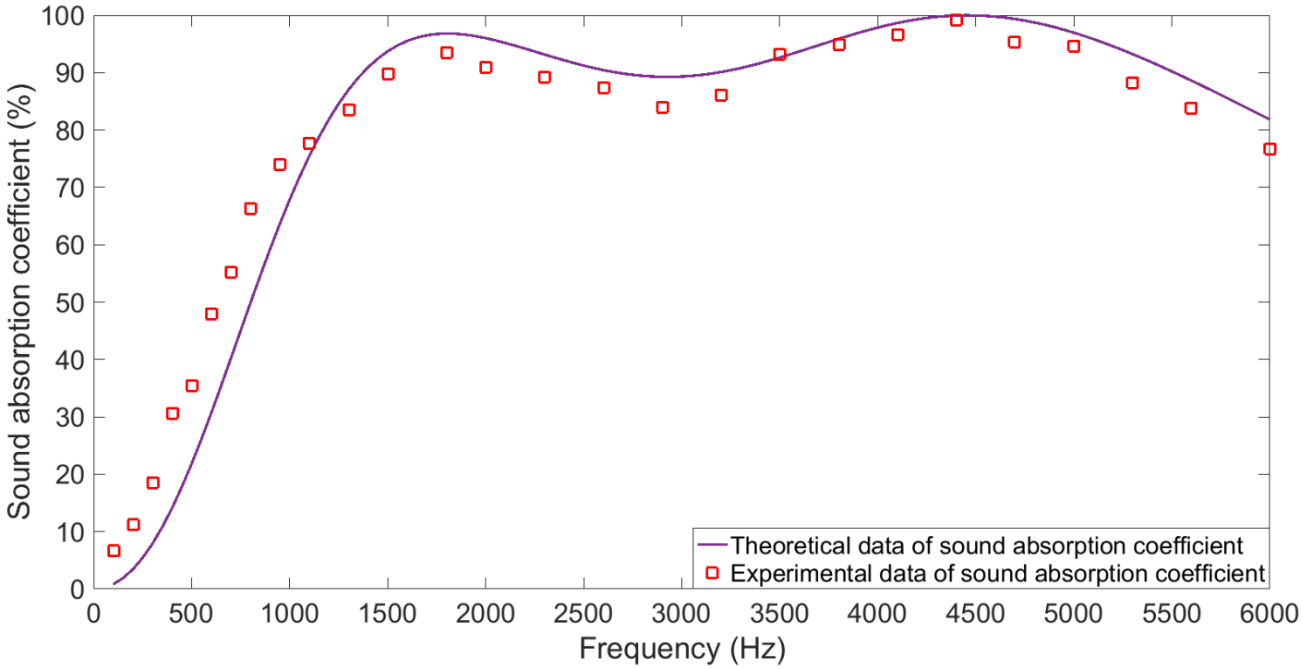

(d) Standardized multilayer microperforated panel with 4 layers

Fig. 6. Comparisons of sound absorption coefficients of the standardized multilayer microperforated panels obtained in theoretical calculation and those achieved in actual experiment

Table. 6 Absolute deviations between the results obtained in experiment and those achieved in theory

Deviations \ layers	1 layer	2 layers	3 layers	4 layers
Maximum	7.7122%	16.9958%	21.2889%	17.3309%
Minimum	0.5425%	0.1098%	0.1292%	0.6770%
Average	3.2684%	6.2108%	8.4403%	6.4272%

6. Conclusions

Optimization of geometric parameters of the proposed standardized multilayer microperforated panel with finite dimension was conducted in this study. Through structural design, theoretical modeling, parameter optimization, finite element simulation, and experimental validation, a novel method to develop sound absorber with finite dimension for high sound absorption performance was proposed, and the following conclusions were achieved from the research results.

(1) Standardized multilayer microperforated panel with finite dimension was proposed and designed, which aimed to improve its practicability and effectiveness. Meanwhile, the pivotal geometric parameters, which affected the sound absorption performance, were analyzed and summarized.

(2) Through constructing the theoretical model according to the Maa's theory, numerical relationship between sound absorption coefficient of the standardized multilayer microperforated panel and its geometric parameters were obtained, which supplied theoretical basis for the optimization process.

(3) Optimal geometric parameters for the standardized multilayer microperforated panel with layer number from 1 to 8 were obtained by the cuckoo search algorithm when the finite dimension was 30 mm, and the corresponding optimal average sound absorption coefficients in the frequency range of 100-6000 Hz were 69.79%, 79.40%, 82.54%, 82.62%, 82.74%, 83.18%, 83.43%, and 83.57%, respectively. The results indicated that the sound absorption performance of the sound absorber could

be improved by optimization of its geometric parameters.

(4) The simulation results obtained by the model constructed according to the finite element method were consistent with those achieved in the theoretical modeling, and the absolute deviations were reduced in 2.5% and their average was 0.3415%, which preliminarily verified accuracy of the optimal geometric parameters.

(5) The actual sound absorption coefficients of the proposed standardized multilayer microperforated panels fabricated by laser beam machining of the spring steels were detected based on the standing wave method, and the experimental results were consistent with the theoretical results, which further validated accuracy of the optimization process. The actual average sound absorption coefficients of the standardized multilayer microperforated panels with layer numbers from 1 to 4 in the frequency range of 100-6000 Hz were 57.45%, 70.85%, 71.99%, and 72.28%, respectively, which indicated that optimization of geometric parameters was effective and impactful to improve sound absorption performance of the sound absorber and promote its practical application.

(6) The improvement of average sound absorption coefficient in 100-6000 Hz is not obvious when the layer number increases from 2 to 4, no matter for the theoretical data, the simulation data, or the experimental data. The research results indicated that it was necessary to balance sound absorption performance and manufacturing cost of the standardized multilayer microperforated panel, which was a critical step to develop practical sound absorption product.

Acknowledgements

This work was supported by a grant from National Natural Science Foundation of China (Grant No. 51505498), a grant from Natural Science Foundation of Jiangsu Province (Grant No. BK20150714), and a grant from National Key R & D Program of China (Grant No. 2016YFC0802900). Xinmin

Shen was grateful for support from the Hong Kong Scholars Program (No. XJ2017025).

References

[1] Maa, D. Y. (**1975**). "Theory and design of microperforated panel sound-absorbing constructions," Sci. Sin. **18(1)**, 55-71.

[2] Maa, D. Y. (**1988**). "Design of microperforated panel constructions," Acta Acust. **13(3)**, 174-180.

[3] Chiang, Y. K., and Choy, Y. S. (**2018**). "Acoustic behaviors of the microperforated panel absorber array in nonlinear regime under moderate acoustic pressure excitation," J. Acoust. Soc. Am. **143(1)**, 538-549.

[4] Bansod, P. V., Teja, T. S., and Mohanty, A. R. (**2017**). "Improvement of the sound absorption performance of jute felt-based sound absorbers using microperforated panels," J. Low. Freq. Noise. V. A. **36(4)**, 376-389.

[5] Okuzono, T., and Sakagami, K. (**2015**). "Room acoustics simulation with single-leaf microperforated panel absorber using two-dimensional finite-element method," Acoust. Sci. & Tech. **36(4)**, 358-361.

[6] Asdrubali, F., and Pispola, G. (**2007**). "Properties of transparent sound-absorbing panels for use in noise barriers," J. Acoust. Soc. Am. **121(1)**, 214-221.

[7] Xi, Q., Choy, Y. S., Cheng, L., and Tang, S. K. (**2016**). "Noise control of dipole source by using microperforated panel housing," J. Sound Vib. **362**, 39-55.

[8] Huang, S. B., Li, S. M., Wang, X., and Mao, D. X. (**2017**). "Microperforated absorbers with incompletely partitioned cavities," Appl. Acoust. **126**, 114-119.

[9] Tayong, R. B., Manyo, J. A. M., Siryabe, E., and Ntamack, G. E. (**2018**). "On the simultaneous inversion of microperforated panels' parameters: Application to single and double air-cavity backed

systems," J. Acoust. Soc. Am. **143(4)**, 2279-2288.

[10] Sui, L. Q., Zhao, X. D., and Zhu, R. Y. (**2006**). "Multilayer Microperforated Structure Optimization Design Using Genetic Algorithm," Noise and Vibration Control **26(2)**, 49-52.

[11] Zhang, X. J., and Zhao, X. D. (**2008**). "Multilayer Micro Perforated Panel Optimization Design," Audio Engineering **32(2)**, 71-74.

[12] Liu, Z. Q., Zhan, J. X., Fard, M., and Davy, J. L. (**2017**). "Acoustic properties of multilayer sound absorbers with a 3D printed microperforated panel," Appl. Acoust. **121**, 25-32.

[13] Zhou, H. A., Wang, X. M., Wu, H. Y., and Meng, J. B. (**2017**). "The vibroacoustic response and sound absorption performance of multilayer, microperforated rib-stiffened plates," Acta. Mech. Sin. **33(5)**, 926-941.

[14] Maa, D. Y. (**1998**). "Potential of microperforated panel absorber," J. Acoust. Soc. Am. **104(5)**, 2861-2866.

[15] Maa, D. Y. (**1997**). "General theory and design of microperforated-panel absorbers," Chin. J. Acoust. **16(3)**, 193-202.

[16] Maa, D. Y., and Liu, K. (**2000**). "Sound absorption characteristics of microperforated absorber for random incidence," Acta Acust. **25(4)**, 289-296.

[17] Yang, X. S., and Deb, S. (**2013**). "Multiobjective cuckoo search for design optimization," Comput. Oper. Res. **40(6)**, 1616-1624.

[18] Yang, X. S., and Deb, S. (**2014**). "Cuckoo search: recent advances and applications," Neural. Comput. & Applic. **24(1)**, 169-174.

[19] Ouaarab, A., Ahiod, B., and Yang, X. S. (**2014**). "Discrete cuckoo search algorithm for the travelling salesman problem," Neural. Comput. & Applic. **24(7-8)**, 1659-1669.

[20] Yang, X. C., Bai, P. F., Shen, X. M., To, S., Chen, L., Zhang, X. N., and Yin, Q. (**2019**). "Optimal design and experimental validation of sound absorbing multilayer microperforated panel with constraint conditions," Appl. Acoust. **146**, 334-344.

[21] Onen, O., and Caliskan M. (**2010**). "Design of a single layer microperforated sound absorber by finite element analysis," Appl. Acoust. **71(1)**, 79-85.

[22] Carbajo, J., Ramis, J., Godinho, L., Amado-Mendes, P., and Alba J. (**2015**). "A finite element model of perforated panel absorbers including viscothermal effects," Appl. Acoust. **90(1)**, 1-8.

[23] Gaudreau, M. A., Sgard, F., Laville, F., and Nélisse, H. (**2017**). "A finite element model to improve noise reduction based attenuation measurement of earmuffs in a directional sound field," Appl. Acoust. **119**, 66-77.

[24] Carillo, K., Sgard, F., and Doutres, O. (**2018**). "Numerical study of the broadband vibro-acoustic response of an earmuff," Appl. Acoust. **134**, 25-33.

[25] Bai, P. F., Shen, X. M., Zhang, X. N., Yang, X. C., Yin, Q., and Liu, A. X. (**2018**). "Influences of Compression Ratios on Sound Absorption Performance of Porous Nickel-Iron Alloy," Metals **8**, 539.

[26] Zhao, X. D., and Fan, X. Q. (**2015**). "Enhancing low frequency sound absorption of microperforated panel absorbers by using mechanical impedance plates," Appl. Acoust. **88**, 123-128.

[27] Bai, P. F., Yang, X. C., Shen, X. M., Zhang, X. N., Li, Z. Z., Yin, Q., Jiang, G. L., and Yang F. (**2019**). "Sound absorption performance of the acoustic absorber fabricated by compression and microperforation of the porous metal," Mater. Des. **167**, 107637.

[28] Yang, X. C., Peng, K., Shen, X. M., Zhang, X. N., Bai, P. F., and Xu, P. J. (**2017**). "Geometrical and dimensional optimization of sound absorbing porous copper with cavity," Mater. Des. **131**, 297-306.

[29] Lee, D. H., and Kwon, Y. P. (**2004**). “Estimation of the absorption performance of multiple layer perforated panel systems by transfer matrix method,” J. Sound. Vib. **278(4-5)**, 847-860.

[30] Zhao, X. D., Hu, P., and Sun, P. (**2012**). “The comparative analyses of the calculation methods for absorptivity of multilayer microperforated panel absorbers,” J. Appl. Acoust. **31(3)**, 196-201.

[31] Verdière, K., Panneton, R., and Elkoun, S. (**2013**). “Transfer matrix method applied to the parallel assembly of sound absorbing materials,” J. Acoust. Soc. Am. **134(6)**, 4648-4658.

[32] Bansod, P. V., and Mohanty, A. R. (**2016**). “Inverse acoustical characterization of natural jute sound absorbing material by the particle swarm optimization method,” Appl. Acoust. **112**, 41-52.

[33] Yildiz, A. R. (**2013**). “Cuckoo search algorithm for the selection of optimal machining parameters in milling operations,” Int. J. Adv. Manuf. Technol. **64(1-4)**, 55-61.